

Role of c -axis field components in making the transport $E(J)$ characteristics of $(\text{Bi,Pb})_2\text{Sr}_2\text{Ca}_2\text{Cu}_3\text{O}_x$ tapes insensitive to the direction of field within the tape plane

H. S. Edelman^{a)} and D. C. Larbalestier^{b)}

Applied Superconductivity Center and Department of Physics, University of Wisconsin–Madison, Madison, Wisconsin 53706

(Received 9 October 1997; accepted for publication 27 January 1998)

We report extended (over four decades) electric field versus current density characteristics of $(\text{Bi,Pb})_2\text{Sr}_2\text{Ca}_2\text{Cu}_3\text{O}_{10}$ tapes in magnetic fields applied along each of the three principal tape axes at 77 K, and along the two principal axes in the tape plane at 4.2 K. The characteristics are almost independent of field direction in the tape plane at both temperatures. Similar insensitivity of the critical current to magnetic field direction observed in other polycrystalline high temperature superconductors has been ascribed to the percolative nature of current flow, while the insensitivity in $(\text{Bi,Pb})_2\text{Sr}_2\text{Ca}_2\text{Cu}_3\text{O}_{10}$ (2223) films and $\text{Bi}_2\text{Sr}_2\text{CaCu}_2\text{O}_8$ single crystals has been attributed to c -axis conduction across Josephson junctions. We show that the insensitivity of the critical current density to the field direction of these tapes follows naturally from the fact that the dissipation depends only on the field component lying along the c axis of individual 2223 grains. Lorenz-force driven motion of the pancake vortices that form within each 2223 grain provides a dissipation mechanism that involves only the c -axis components of the field. The angular dispersion of the grains in the tape ensures a c -axis field component in most grains, regardless of the applied field direction. This produces the remarkable insensitivity of $E(J)$ over some four orders of magnitude of the electric field. © 1998 American Institute of Physics. [S0021-8979(98)04309-6]

I. INTRODUCTION

The goal of much development work on $(\text{Bi,Pb})_2\text{Sr}_2\text{Ca}_2\text{Cu}_3\text{O}_{10}$ (2223) tapes is to increase the overall critical current density, $J_C = I_C/A$, where I_C is the critical current and A the cross sectional area of the superconductor. The ability to accomplish this depends strongly on understanding the path taken by current through the tape, the fraction of A utilized by the current, and the dissipation processes associated with current flow. Two contrasting models of current flow postulate different paths with potentially different loss mechanisms. In the ‘‘brick wall model’’¹ grain-to-grain current transfer occurs along the common c axis of stacked grains that are separated by (001) twist boundaries.² These twist boundaries form at the weak Bi–O double layer, two of which are found in each unit cell. There is now strong evidence that these double layers form weak links.³ However, the brick wall model proposes a way in which they may still carry high current densities in strong fields. By contrast, the ‘‘railway switch model’’⁴ treats the current as flowing along a - b planes and crossing low angle tilt boundaries between grains whose a - b planes are slightly inclined with respect to one another. The presence of tilt boundaries results from the angular dispersion of the c axis of grains within a tape.

The above two models emphasize different crystallographic directions of current flow and thus suggest different strategies for optimizing the grain-to-grain connectivity. It is widely recognized that multiple parallel current paths exist in real tapes.^{5–8} Magneto-optical images provide direct evidence of these percolative current paths,⁹ but generally lack the spatial resolution to distinguish between particular percolation paths. Such percolative current flow means that the local current vector is often quite different from the macroscopic one. Any local segments for which the field \mathbf{H} and the current density \mathbf{J} are not fully orthogonal may have a reduced Lorenz force and a higher J_C . In both Chevrel-phase wires¹⁰ and $\text{YBa}_2\text{Cu}_3\text{O}_{7-\delta}$ tapes,¹¹ it has been shown that the ratio $J_C(\mathbf{H}\parallel\mathbf{J})/J_C(\mathbf{H}\perp\mathbf{J})$ increases as the connectivity of the sample improves, consistent with the view that strongly percolative current flow always has a significant $(\mathbf{H}\perp\mathbf{J})$ component, whatever the macroscopic orientation of \mathbf{H} and \mathbf{J} .

A complication in the interpretation of such different data sets is the dimensionality of the vortices. In $\text{YBa}_2\text{Cu}_3\text{O}_{7-\delta}$ and the Chevrel phases, vortices are line objects, but vortex lines decompose into pancake vortices that lie within the CuO_2 planes in the much more anisotropic BSCCO compounds. Such pancake vortices are only weakly coupled to each other across the Bi–O layers. The impact of the breakup of vortex lines into chains of pancakes is best illustrated by previous work on single crystal 2223 films and $\text{Bi}_2\text{Sr}_2\text{CaCu}_2\text{O}_8$ (2212) single crystals, which are free of the complicating effects of large scale percolative current flow seen in 2223 tapes. Yamasaki *et al.*¹² found that J_C measured for transport within the a - b plane of 2223 films did not

^{a)}Now at Seagate Technology, 7801 Computer Ave., Minneapolis, MN 55435.

^{b)}Also at the Department of Materials Science and Engineering; electronic mail: larbales@engr.wisc.edu

depend on the direction of magnetic field, H , applied within the a - b plane for $H < 2$ T. However, J_C was slightly higher for $2 \leq H < 15$ T when H was applied in the macroscopic ‘‘Lorenz-force free’’ configuration, $\mathbf{H} \parallel \mathbf{J}$. Other groups have measured the flux-flow resistivity, ρ , of 2212 single crystals as a function of field direction for current density, J , applied both within the a - b planes¹³ and along the c axis.¹⁴ Both ρ_{ab} and ρ_c reached the maxima for field applied along the c axis, and both were insensitive to the orientation of fields ≤ 5 T lying in the a - b plane. Kes *et al.*¹⁵ interpreted their ρ_{ab} data¹³ by treating 2212 as a stack of superconducting CuO_2 planes separated by normal spaces into which H penetrates freely. The only vortices in this two-dimensional (2D) limit are pancake vortices, which lie within the CuO_2 planes. The electric field, $E(J_{ab})$, then depends on the density of pancake vortices, which is determined by the magnitude of the c -axis field component, regardless of the nominal field direction. The in-plane resistivity (ρ_{ab}) resulting from motion of pancake vortices under the Lorenz force should be independent of H_{ab} , as reported in Ref. 13, if pancake vortices in adjacent layers are not coupled together. Other authors^{2,14,16} have addressed the consequences of such a layered structure for the c -axis critical current by treating ρ_c in terms of conduction through a stack of Josephson junctions.¹⁷

Because the nature of the current path is so vital to understanding the ultimate current-carrying limits of 2223 tapes, we tried to analyze some of the above complexities by measuring the extended electric field versus current density characteristics, $E(J)$, of 2223 tapes in different field directions at both 77 and 4.2 K. We interpret our data by extending the interpretation of Kes *et al.*¹⁵ to include polycrystalline samples with misaligned grains and to allow for some coupling between vortices in adjacent layers. Although we are certain that current flow is percolative in our tapes since percolation was directly observed in some of this set by magneto-optical imaging,⁹ we deduce that comparison of $J_c(\mathbf{H} \parallel \mathbf{J})/J_c(\mathbf{H} \perp \mathbf{J})$ characteristics does not yield further useful current-path information because dissipation is controlled by local pancake vortex motion, whatever the macroscopic directions of \mathbf{H} and \mathbf{J} . This accounts for the remarkable insensitivity of the measured $E(J)$ characteristics observed over a wide range of E , H , and T space.

II. EXPERIMENT DETAILS AND RESULTS

The tape whose characteristics are reported here was fabricated by an oxide powder-in-tube method using a ‘‘two powder’’ starting material.¹⁸ Thermomechanical processing raised J_C ($1 \mu\text{V}/\text{cm}$, 77 K, 0 T) of the tape to $14.5 \text{ kA}/\text{cm}^2$ by increasing its core density and aligning the CuO_2 layers within the plane of the tape.¹⁹ Other tapes of this type exhibited J_C up to $23 \text{ kA}/\text{cm}^2$.²⁰ Measurements were performed with samples immersed in liquid He or N_2 to minimize any variation in sample temperature over the extended voltage range of the measurements. The magnetic field was aligned to each tape axis with a $\pm 3^\circ$ tolerance that was small relative to the 10° – 15° angular dispersion of the c axes of the BSCCO grains within the tape. Central voltage taps from the four in-line probes were connected to the preamplifier inputs

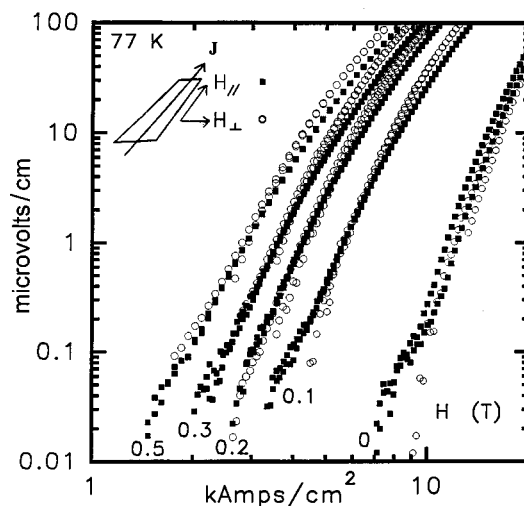


FIG. 1. $E(J)$ characteristics of a $(\text{Bi,Pb})_2\text{Sr}_2\text{Ca}_2\text{Cu}_3\text{O}_{10}$ tape at 77 K for fields applied in the tape plane either parallel or perpendicular to the nominal current direction. The two field directions have an equivalent effect on $E(J)$. Electric field values for both increasing and decreasing current are shown for each magnetic field. The data labeled ‘‘0’’ represent two independent measurements of $E(J)$ at $H=0$ T. Current sharing with the Ag sheath causes the curvature at high E .

with continuous copper wire. This reduced the variation in baseline thermoelectric voltage over the 6 mm between taps to $\pm 3 \text{ nV}$ ($\pm 5 \times 10^{-3} \mu\text{V}/\text{cm}$), which was generated by the ~ 300 K temperature difference across the voltage circuit. Figure 1 shows the electric field as a function of J in the tape at 77 K for several values of magnetic field from 0 to 0.5 T, applied within the tape plane, either parallel or perpendicular to the current. A very striking result of Fig. 1 is that the effect of H on the curves is nearly the same for the two orthogonal field directions over four decades of electric field. Four other tapes processed under different heat treatment and pressing conditions exhibited the same behavior.

Figure 2 shows similar measurements at 4.2 K. At this temperature $E(J)$ still appears to be approximately independent of field direction within the tape plane for $H \leq 3$ T. For $H=10$ T in the tape plane, there is more dissipation at high electric fields for $\mathbf{H} \perp \mathbf{J}$ than for $\mathbf{H} \parallel \mathbf{J}$, while $E(J)$ is the same for both cases at low electric fields. This is very similar to the disparity in J_C values for the two field orientations that appeared only at magnetic fields above 2 T in the 2223 films of Yamasaki *et al.*¹² The faster rise in $E(J)$ at high electric fields for $\mathbf{H} \perp \mathbf{J}$ than for $\mathbf{H} \parallel \mathbf{J}$ is most apparent at 4.2 K and 10 T, but it is nonetheless discernible in all the data of Figs. 1 and 2 taken at finite magnetic fields. Such an effect suggests that either the dissipation mechanism or the current path changes with electric field. Indeed, magneto-optical images taken by Pashitski *et al.* of a tape similar to the one in this study⁹ show that the length scale of percolative current loops increases with increasing E and that the transport current also spreads into more of the cross section as the electric field increases. Figure 2 also shows a small offset in $E(J)$ at low electric fields at 4.2 K between the two magnetic field orientations for 0.3 and 1.0 T. The offset is absent at 77 K (Fig. 1) and we did not look for it on other samples. Figure 3 shows characteristics of the same tape at 77 K as a function

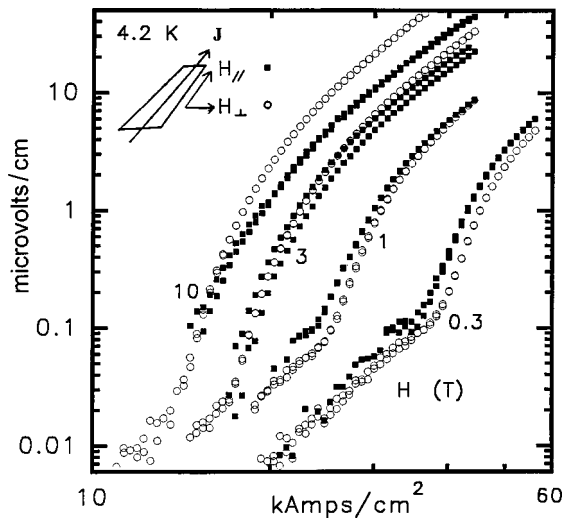


FIG. 2. $E(J)$ characteristics at 4.2 K for the same tape and field directions as in Fig. 1. The two field directions in the tape plane have an equivalent effect on $E(J)$, except at $H=10$ T and $E=1 \mu\text{V}/\text{cm}$. The x axis is shifted to higher J than in Fig. 1. The shallower slope at low E may result from a small component of c -axis current.

of H applied orthogonal to the tape plane (parallel to the nominal c axis). It is apparent that the predominantly c -axis field has a much more pronounced effect on $E(J)$ than does the corresponding value of H applied within the tape plane at 77 K (Fig. 3 vs Fig. 1).

III. DISCUSSION

In order to interpret the $E(J)$ curves it is essential to recognize that the grains in these tapes are not perfectly aligned. Their angular dispersion results in c -axis field components in most grains, even when the macroscopic field vector, H , lies in the tape plane. These c -axis components generate pancake vortices, whatever the nominal field direction. We consider the case of a current introduced into the

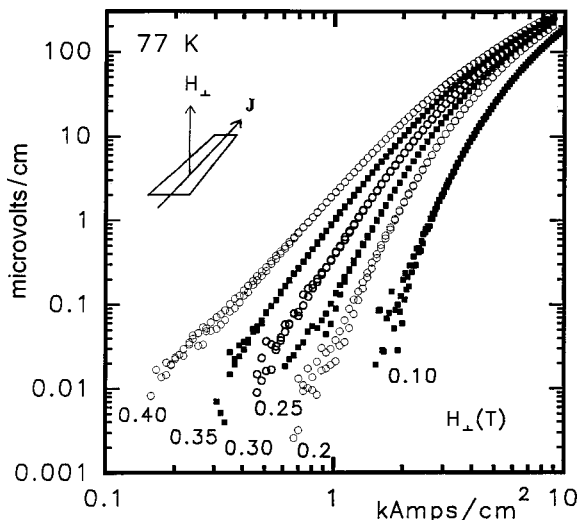


FIG. 3. $E(J)$ characteristics at 77 K for the same tape as in Figs. 1 and 2, in a field applied orthogonal to the tape plane. The narrower range of orthogonal field displaces the curves over more decades of J than the wider range of in-plane field in Fig. 1.

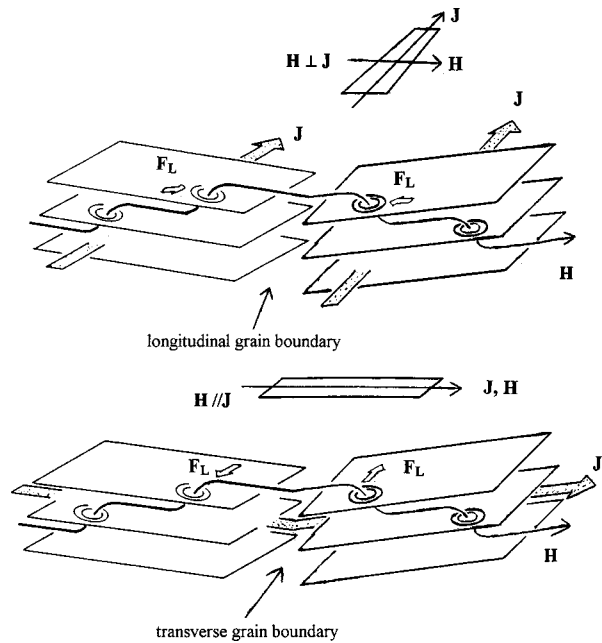


FIG. 4. Depicted is a different pair of adjacent grains for the two configurations of \mathbf{J} and \mathbf{H} within the tape plane. Within each pair the grains have opposite tilts so that their c -axis field components and associated pancake vortices are of opposite polarity. In the upper drawing $\mathbf{H}\perp\mathbf{J}$ and the Lorentz force pushes pancake vortices along the strings connecting them. In the lower drawing $\mathbf{H}\parallel\mathbf{J}$ and the Lorentz force pushes them orthogonal to the strings. In both cases the vortices move in opposite directions in the two grains but generate \mathbf{E} in the direction of \mathbf{J} in both grains. Only $\mathbf{H}\parallel\mathbf{J}$ shears the fluxons at the grain boundary and requires flux cutting to maintain vortex motion and the corresponding steady-state electric field, \mathbf{E} .

plane of the tape that follows the local a - b planes through each grain. Such a current path was proposed by Hensel *et al.*⁴ in the context of the railway switch model and later was corroborated experimentally by Cho *et al.*¹⁷ Figure 4 depicts two pairs of neighboring grains. The grains in each pair are slightly misaligned, both with respect to each other and to the tape plane. A macroscopic field, H , applied parallel to the tape plane creates the vortex structure shown in Fig. 4, because of the c -axis field components that are present in any grain which is not perfectly aligned with the tape plane. In both pairs of grains, J is parallel to the long axis of the tape, and the two grains are separated by a boundary plane that is nominally perpendicular to H . Locally the field lies within the Bi-O double layers, except where it crosses a CuO_2 plane and forms a pancake vortex as indicated. For field applied in the plane of the tape and perpendicular to its long axis, i.e., macroscopic ($\mathbf{H}\perp\mathbf{J}$), the Lorentz force on the pancake vortices $\mathbf{F}_L \sim \mathbf{J}_{ab} \times \mathbf{B}_c$ acts in the a - b plane orthogonal to the vortex field, and in a direction orthogonal to the local \mathbf{J} , i.e., along the a - b component of H (Fig. 4). The pancake vortices respond by moving parallel to the Josephson strings that connect vortices in adjacent CuO_2 layers. Their speed is determined by the thermal activation rate in the flux creep limit, and by a Bardeen-Stephen type of viscosity in the flux flow regime. The Lorentz force generates opposite velocities for the two vortex polarities, and both induce an electric field²¹ $\mathbf{E} \sim \mathbf{B} \times \mathbf{v} \sim \mathbf{B} \times (\mathbf{J} \times \mathbf{B})$, which

is in the direction of J . Any Lorenz force on the Josephson strings lying between the CuO_2 layers acts in the c direction and is opposed by strong intrinsic pinning.

For fields applied along the long tape axis, i.e., macroscopic ($\mathbf{H}\parallel\mathbf{J}$), the Lorenz force on the pancake vortices is still within the a - b plane and orthogonal to J , and is thus also orthogonal to the Josephson string (a - b) component of H . There is now no force on the strings themselves, since these are parallel to J . A block of grains with a - b planes tilted in the same sense relative to the applied field will contain pancake vortices of only one polarity. The boundaries of such a block are defined by a transition to grains of opposite tilt with respect to H . Pancake vortices in these adjacent grains will have the other polarity, and the Lorenz force will push pancake vortices on opposite sides of the block boundary in opposite directions, as shown in Fig. 4. If the pancake vortices are coupled by Josephson strings that follow H_{ab} , the resulting fluxon will form kinks at the grain boundaries between oppositely tilted blocks. If the fluxons are weakly coupled across these boundaries and the kinks become big enough, the fluxon lattice on one side of a boundary can shift position by one lattice parameter relative to the fluxon lattice on the other side, in a version of flux cutting.²² This motion of flux, through fluxon distortion and cutting, can continue indefinitely and will induce a steady-state electric field. As in the macroscopic ($\mathbf{H}\perp\mathbf{J}$) case, the opposite velocities of the two vortex polarities both produce electric fields in the direction of J , while strings moving in opposite directions can produce only electric fields that oppose one another. If the flux lattice is soft enough that the process is limited by the pinning of pancake vortices, as it is for the macroscopic ($\mathbf{H}\perp\mathbf{J}$) case, rather than by the collective elastic interactions of the fluxons, the induced electric field will be similar for the two cases. Figures 1 and 2 show that the two dissipative processes generate very similar $E(J)$ curves over a large range of E , H , and T space.

There is one important feature of the extended $E(J)$ curves in Figs. 1–3 that supports this interpretation in terms of current flow along a - b planes rather than along the c axis. Figures 1–3 do not show any low E , ohmic region that shifts to lower J with applied field. Such ohmic regions are characteristic of the $V(J)$ curves measured along the c axis of 2212 single crystals²³ and they are occasionally observed in transport at 4.2 K along damaged 2223 tapes.^{24,25} By contrast, our curves are very similar in shape to the extended $E(J)$ curves measured by Yamasaki *et al.*²⁶ with J in the plane of 2223 films. The similarity of our tape data to film data suggests that the dissipation density, $\mathbf{E}\cdot\mathbf{J}$, is associated with transport along a - b planes in tapes, just as it is in films. Figure 2 does reveal a shallower $E(J)$ slope at low E , although not shallow enough to be ohmic. The anomalous slope may become visible above the effect of thermally activated vortex motion only at low temperature, or it may indicate damage to the tape during the final cooling to 4.2 K. In either case the pancake vortex dissipation mechanism described above would still apply to the data in Fig. 2 for $E \geq 0.1 \mu\text{V}/\text{cm}$.

IV. SUMMARY

We have presented measurements of the magnetic-field dependent dissipation in polycrystalline 2223 tapes for currents applied within the tape plane both at 77 and 4.2 K. The dissipation is much stronger for \mathbf{H} orthogonal to the plane than for H within the plane, but is approximately the same for in-plane fields whether they are parallel or perpendicular to J . We show that the observed field dependence follows naturally from Lorenz-force driven motion of the pancake vortices that carry the c -axis field component, and cutting of the flux that links these vortices across grain boundaries. This process can occur with either direct or percolative current flow along the a - b planes. Thus dissipation is entirely controlled by the magnetic-field component lying along the local c axis of each grain. Because of angular grain dispersion, this component is nonzero in most grains, even for fields applied within the tape plane. Our model extends an earlier interpretation by Kes *et al.*¹⁵ of ρ_{ab} data on 2212 films¹³ by incorporating the effects of misaligned grains and allowing for modest coupling between vortices in adjacent layers.

ACKNOWLEDGMENTS

The authors wish to thank S. E. Dorris for the starting BSCCO powder and J. A. Parrell for processing the tapes. This work was supported by EPRI.

- ¹A. P. Malozemoff, in *Superconductivity and its Applications*, edited by Y. H. Kao *et al.* (AIP, New York, 1992), p. 6; L. N. Bulaevskii, J. R. Clem, L. I. Glazman, and A. P. Malozemoff, *Phys. Rev. B* **45**, 2545 (1992).
- ²L. L. Daemen, L. N. Bulaevskii, M. P. Maley, and J. Y. Coulter, *Phys. Rev. B* **47**, 11 291 (1993).
- ³P. Kleiner and R. Muller, *Phys. Rev. B* **49**, 1327 (1994).
- ⁴B. Hensel *et al.*, *Physica C* **205**, 329 (1993); B. Hensel, G. Grasso, and R. Flukiger, *Phys. Rev. B* **51**, 15 456 (1995).
- ⁵M. Dhallé, M. Cuthbert, M. D. Johnson, J. Everett, R. Flükiger, S. X. Dou, W. Goldacker, T. Beales, and A. D. Caplin, *Semicond. Sci. Technol.* **10**, 21 (1997).
- ⁶J. Horvat, Y. C. Guo, and S. X. Dou, *Physica C* **271**, 59 (1996).
- ⁷D. C. Larbalestier, in *Proceedings of HTS Workshop on Physics, Materials, and Applications*, edited by D. Gubser (World Scientific, Singapore, 1996), p. 41.
- ⁸D. C. Larbalestier, *IEEE Trans. Appl. Supercond.* **7**, 90 (1997).
- ⁹A. E. Pashitski, A. Polyanskii, A. Gurevich, J. A. Parrell, and D. C. Larbalestier, *Appl. Phys. Lett.* **67**, 2720 (1995).
- ¹⁰H. Yamasaki, M. Umeda, S. Kosaka, Y. Kimura, T. C. Willis, and D. C. Larbalestier, *J. Appl. Phys.* **70**, 1606 (1991).
- ¹¹H. Safar, S. Foltyn, H. Kung, M. P. Maley, J. O. Willis, P. Arendt, and X. D. Wu, *Appl. Phys. Lett.* **68**, 1853 (1996).
- ¹²H. Yamasaki *et al.*, *J. Appl. Phys.* **72**, 2951 (1992).
- ¹³Y. Iye, S. Nakamura, and T. Tamegai, *Physica C* **159**, 433 (1989).
- ¹⁴K. Kadowaki, Y. Songliu, and K. Kitazawa, *Semicond. Sci. Technol.* **7**, 519 (1994).
- ¹⁵P. H. Kes, J. Aarts, V. M. Vinokur, and C. J. van der Beck, *Phys. Rev. Lett.* **64**, 1063 (1990).
- ¹⁶K. E. Gray and D. H. Kim, *Phys. Rev. Lett.* **70**, 1693 (1993).
- ¹⁷J. H. Cho *et al.*, *Appl. Phys. Lett.* **64**, 3030 (1994).
- ¹⁸S. E. Dorris, B. C. Prorok, M. T. Lanagan, S. Sinha, and R. B. Poeppel, *Physica C* **212**, 66 (1993).
- ¹⁹J. A. Parrell, S. E. Dorris, and D. C. Larbalestier, *Adv. Cryog. Eng.* **40**, 193 (1994); Y. E. High *et al.*, *Physica C* **220**, 81 (1994).
- ²⁰S. E. Dorris, B. C. Prorok, M. T. Lanagan, N. B. Browning, M. R. Hagan, J. A. Parrell, Y. Feng, A. Umezawa, and D. C. Larbalestier, *Physica C* **223**, 163 (1994).
- ²¹M. Tinkham, in *Introduction to Superconductivity* (Krieger, Malabar, FL, 1980), p. 158.

²²A. M. Cambell and J. E. Evetts, *Adv. Phys.* **21**, 199 (1972).

²³J. H. Cho, M. P. Maley, S. Fleshler, A. Lacerda, and L. N. Bulaevskii, *Phys. Rev. B* **50**, 6493 (1994).

²⁴Y. Fukumoto, Q. Li, Y. L. Wang, M. Suenaga, and P. Haldar, *Appl. Phys. Lett.* **66**, 1827 (1995).

²⁵M. Polak, W. Zhang, J. Parrell, X. Y. Cai, A. Polyanskii, E. E. Hellstrom, D. C. Larbalestier, and M. Majoros, *Supercond. Sci. Technol.* **10**, (1997).

²⁶H. Yamasaki, K. Endo, S. Kosaka, M. Umeda, S. Yoshida, and K. Kajimura, *Phys. Rev. B* **50**, 12 959 (1994).